Tuning the van der Waals Interaction of Graphene with Molecules via Doping

Felix Huttmann,[1,*] Antonio J. Martínez-Galera,[1] Vasile Caciuc,[2] Nicolae Atodiresei,[2,†] Stefan Schumacher,[1] Sebastian Standop,[1] Ikutaro Hamada,[3] Tim O. Wehling,[4] Stefan Blügel,[2] and Thomas Michely[1]

[1]*II. Physikalisches Institut, Universität zu Köln, Zülpicher Straße 77, 50937 Köln, Germany*

[2]*Peter Grünberg Institute and Institute for Advanced Simulation, Forschungszentrum Jülich, 52428 Jülich, Germany*

[3]*International Center for Materials Nanoarchitectonics (WPI-MANA) and Global Research Center for Environment and Energy based on Nanomaterials Science (GREEN), National Institute for Materials Science, 1-1 Namiki, Tsukuba 305-0044, Japan*

[4]*Bremen Center for Computational Material Science (BCCMS), Universität Bremen, Am Fallturm 1a, 28359 Bremen, Germany*

(Received 7 September 2015; published 1 December 2015)

We use scanning tunneling microscopy to visualize and thermal desorption spectroscopy to quantitatively measure that the binding of naphthalene molecules to graphene, a case of pure van der Waals interaction, strengthens with n and weakens with p doping of graphene. Density-functional theory calculations that include the van der Waals interaction in a seamless, *ab initio* way accurately reproduce the observed trend in binding energies. Based on a model calculation, we propose that the van der Waals interaction is modified by changing the spatial extent of graphene's π orbitals via doping.

DOI: 10.1103/PhysRevLett.115.236101 PACS numbers: 68.65.Pq, 68.37.Ef, 68.43.Vx

One of the key properties of graphene is the wide-range tunability of its Fermi level and corresponding charge carrier concentration, which can be controlled by a gate electrode [1], substitutional doping [2], adsorption [3,4], or charge transfer from a supporting material or intercalation layer [5–8]. The tunability of the Fermi level through the otherwise rigid band structure results from the material being atomically thin and having a negligible density of states near the Dirac point.

In recent years, interest has arisen in using this tunability to control adsorption. For the case of ionic adsorbates, Brar *et al.* [9] demonstrated a dependence of the ionization state of a Co adatom on the graphene Fermi-level position, and Schumacher *et al.* [10] found a doping-dependent binding energy E_b of ionic adsorbates to graphene, with a shift in E_b on the order of the shift in the Fermi level induced by doping. For the case of radicals, Wehling *et al.* [11] predict, based on *ab initio* calculations, doping-dependent adsorbate phase transitions for hydrogenated as well as fluorinated graphene, while Huang *et al.* [12] find a stronger binding of isolated H radicals for larger magnitudes of doping.

For the case of van der Waals (vdW) interaction, the effect of the graphene doping level on the binding energy of adsorbates has not yet been explored. This is surprising, given that the adsorption of simple hydrocarbons to graphite or graphene has been used as a model system to study vdW interactions [13–16]. Here, we investigate this case with the help of epitaxial graphene on Ir(111), which can be doped from the back side by the intercalation of highly electropositive (e.g. Cs or Eu) or electronegative (e.g., O) elements into its interface with the substrate, while graphene's other side remains available for the adsorption experiment itself. This strategy not only enables us to achieve large Fermi-level shifts on the order of ± 1 eV, but also to visualize doping-induced binding energy differences by making use of intercalation patterns [10]. Naphthalene is chosen as a test molecule, since its binding to graphene is a pure vdW case that has been studied previously, both experimentally [14] and theoretically [13]. Our experiments are complemented by density-functional theory (DFT) calculations that include the vdW interaction in a seamless, *ab initio* way (for a recent review, see Ref. [17]).

For this paradigmatic case we find, with excellent agreement of experiment and theory, an increase of the vdW binding energy when changing from p to n doping. We identify the mechanism of this binding energy manipulation, which is likely to hold for a broad class of molecular adsorbates and a variety of two-dimensional materials.

The experiments were performed in two variable-temperature scanning tunneling microscopy (STM) systems with base pressures below 1×10^{-10} mbar. Ir(111) was prepared by sputter-anneal cycles, yielding clean terraces with sizes on the order of 100 nm. Well-oriented graphene was prepared by room-temperature ethylene adsorption until saturation, thermal decomposition at 1500 K, and subsequent exposure to 5×10^{-7} mbar of ethylene at 1170 K [18]. Using 600-s ethylene exposure time, a perfectly closed, 1-monolayer (ML) graphene layer was achieved, while with 180 s a partial $\approx$0.9-ML graphene layer resulted. For n doping, Eu was intercalated under 1-ML graphene on Ir(111) at 550 K by exposure to high-purity Eu [19] vapor. For p doping, oxygen was intercalated until saturation under 0.9-ML graphene on Ir(111) at 530 K using a local oxygen pressure of about 2.5×10^{-4} mbar for 600 s. Naphthalene exposure [20] was controlled by a variable leak valve. STM images were taken at 35 K and digitally postprocessed with the WSxM software

[21]. Thermal desorption spectroscopy was performed with a sample heating rate of 1 $\mathrm{K\,s^{-1}}$ by monitoring desorbing naphthalene (molecular mass $m = 128$ u). The sample temperature measurement during thermal desorption measurements with a K-type thermocouple has an absolute error below 3 K with a reproducibility better than 1 K.

The DFT calculations were carried out in the generalized gradient approximation [22] with a kinetic energy cutoff of 500 eV, using the projector-augmented wave method [23] as implemented in the VASP code [24,25]. The ground-state geometry and the corresponding electronic structure were investigated using the nonlocal correlation energy functional vdW-DF2 [26] with a revised [27] Becke (B86b) exchange energy functional [28]. The unit cell comprised (10×10) graphene unit cells on 4 layers of (9×9) Ir(111), either pristine or intercalated by Eu or O.

We start with a discussion of the STM preparations and measurements. Upon intercalation of submonolayer amounts of Eu, a complex pattern of stripes and islands of Eu-intercalated graphene [high (bright)] in coexistence with nonintercalated graphene [low (dark)] emerges, as shown in the STM topograph in Fig. 1(a) and discussed in Ref. [29]. Within the intercalated patches, Eu forms a $p(2 \times 2)$ superstructure and leads to local doping of graphene by -1.36 eV, while the surrounding pristine graphene areas remain hardly doped at $+0.1$ eV [10].

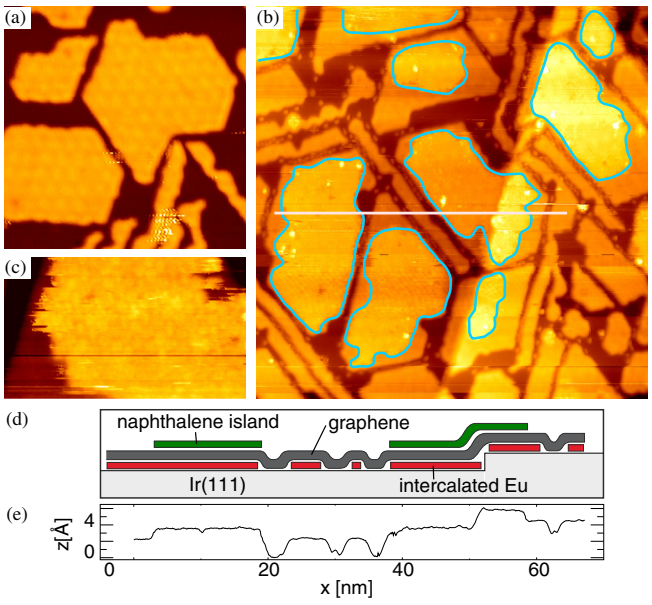

FIG. 1 (color online). (a)–(c): STM topographs imaged at 35 K. (a) Graphene/Ir(111) after intercalation of about half a monolayer coverage of Eu [$(39\ \mathrm{nm})^2$]. (b) Like (a), but with additional submonolayer coverage of naphthalene [$(90\ \mathrm{nm})^2$]. (c) Molecular resolution of a naphthalene island [$(18 \times 11)\ \mathrm{nm}^2$]. (d) Schematic cross section corresponding to the profile in (e). (e) Height profile along the white line indicated in (b).

After the deposition of submonolayer amounts of naphthalene at $T < 50$ K and the subsequent brief annealing to $T = 150$ K, the sample is cooled down again for STM imaging. The corresponding Fig. 1(b) displays additional naphthalene islands (cyan encircled) only on top of Eu-intercalated patches. The profile in Fig. 1(e) taken along the white line in Fig. 1(b) shows that the apparent height of the Eu intercalation island itself stays unchanged at 2 Å, while the naphthalene islands have an apparent height of about 1.3–1.5 Å on top of the Eu-intercalated graphene. The schematic cross section of Fig. 1(d) visualizes the morphology underlying the height profile. Higher-resolution imaging displayed in Fig. 1(c) reveals the molecular resolution of the naphthalene adsorbate layer. Our interpretation is as follows: During annealing, the molecules are highly mobile, diffusing over the surface while sensing local adsorption energy differences. As the sample is cooled down again, the arrangement is frozen and the preferential coverage of intercalated areas by molecules then directly reflects the preferential binding to these areas.

To strengthen our case for the generality of this result, we repeated the experiment, exchanging naphthalene with benzene, and found qualitatively the same results (compare [30]).

In order to quantify the difference in E_b observed in STM, we investigated the thermal desorption of naphthalene from homogeneous graphene layers, i.e., layers that are either entirely pristine or entirely Eu $p(2 \times 2)$ intercalated, rather than the partially intercalated sample employed for STM measurements of Fig. 1. This way, the desorption signal results from a phase-pure sample, avoiding difficulties in the interpretation of the desorption traces.

Figure 2 shows the desorption traces for naphthalene coverages of 1 ML and (2.3 ± 0.2) ML. The low-temperature peak corresponds to desorption from the naphthalene multilayer and is of zeroth order, as seen in the exponential leading edge followed by a sharp drop in

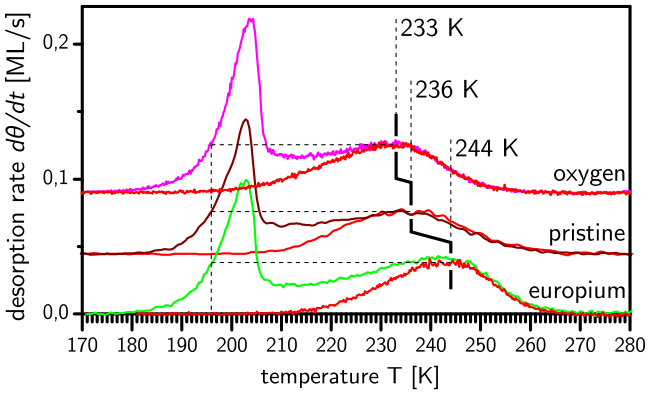

FIG. 2 (color online). Mass spectrometer signal of desorbing naphthalene ($m = 128$ u) while the sample is heated with a ramp rate of 1 K/s in dependence of the intercalant for the coverages of 1 ML and $\approx(2.3 \pm 0.2)$ ML, respectively.

intensity; the high-temperature peak is almost symmetric, indicative of first-order desorption. For pristine graphene, the maximum of the monolayer peak is at $T_{\max} = 236$ K. These findings agree, within the limits of error, with those of Zacharias *et al.* [14] for naphthalene desorption from graphite, which is a hint that the influence of the Ir substrate on the binding of naphthalene to graphene is negligible.

Upon intercalation of Eu $p(2 \times 2)$ (associated with a -1.36 eV graphene doping level), the monolayer peak is shifted up to 244 K, which is evidence for increased $|E_b|$; the position of the multilayer peak is the same as seen in its intercept with the desorption rate at the maximum of the monolayer peak (horizontal dashed lines) at 196 K (left vertical dashed line). As the multilayer peak is not expected to shift, due to the diminishing effect of the substrate with increasing molecular film thickness, its presence provides an integrated temperature calibration.

Using thermal desorption spectroscopy, we also investigated naphthalene desorption from O-intercalated graphene, for which the monolayer $T_{\max}$ is shifted down to 233 K, as shown in Fig. 2. The intercalation of graphene was homogeneous in the case of O intercalation, too, as verified by STM (cf. Ref. [34]), both before and after the thermal desorption measurements [35]. The thermal desorption of naphthalene from two other graphene intercalation systems [Cs and Eu $(\sqrt{3} \times \sqrt{3})$] is analyzed in the Supplemental Material [30]. Altogether, we find a strictly monotonic increase of $|E_b|$, with the Fermi level moving up in the band structure from p to n doping.

To extract E_b from the desorption temperatures, we employed the Redhead method, using the previously determined value of the preexponential factor $\nu = 5 \times 10^{16\pm2}$ Hz [14]. The left part of Table I lists the experimentally determined E_b^{exp} alongside the doping levels E_D^{exp}, which are given in terms of the position of the Dirac cone relative to the Fermi level as determined in angle-resolved photoemission measurements. The experimental error in E_b is about 100 meV, and is dominated by the error of the preexponential factor. However, as the preexponential factor acts equally in the calculation of all E_b, the errors of the differences in E_b for differently doped graphene are dominated by the reproducibility of the temperature measurement; they are, therefore, much smaller—only about 4 meV.

In order to better understand the origin of the observed change in E_b upon intercalation, we have conducted DFT calculations of the naphthalene molecule on non-intercalated as well as O- and Eu-intercalated graphene. Figures 3(a) and 3(b) show the geometries of the calculations for the intercalated systems, while the right part of Table I provides the calculated values for doping level E_D^{theor} and binding energy E_b^{tot}.

The calculated doping level E_D^{theor} has been determined from the shift of graphene's Dirac point against the Fermi level and, thus, should be directly comparable to the value extracted from angle-resolved photoemission. Indeed, we find that the calculated doping levels E_D^{theor} are in reasonable agreement with the experimentally determined E_D^{exp}; in particular, we confirm n doping of graphene by Eu intercalation and p doping of graphene by O intercalation. Qualitatively, the doping is also seen in the charge density difference plots in Figs. 3(c) and 3(d), which give a direct image of charge accumulation (for Eu) and depletion (for O) on the graphene site. These plots also show that charge transfer between the naphthalene molecule and graphene is absent (a Bader analysis [39] yields a charge transfer of less than 0.03 electrons), which is a precondition for using naphthalene adsorbed to graphene as a model for vdW interaction even when graphene is supported on a substrate and doped by intercalation.

Next, we look at the theoretical binding energy, defined as $E_b^{\mathrm{tot}} = E_{\mathrm{sys}}^{\mathrm{tot}} - (E_{\mathrm{surf}}^{\mathrm{tot}} + E_{\mathrm{molec}}^{\mathrm{tot}})$, where $E_{\mathrm{sys}}^{\mathrm{tot}}$ is the total energy of the molecule-surface system, $E_{\mathrm{surf}}^{\mathrm{tot}}$ denotes the total energy of the surface [i.e., the graphene/O/Ir(111), graphene/Ir(111), and graphene/Eu/Ir(111) systems], and $E_{\mathrm{molec}}^{\mathrm{tot}}$ corresponds to the total energy of the naphthalene molecule in the gas phase. As is apparent from Table I, the calculations reproduce the experimentally observed increase in $|E_b|$ rather well when going from naphthalene on O-intercalated graphene, via pristine graphene, to Eu-intercalated graphene.

However, considering absolute numbers, two points have to be noted: First, while graphene is essentially freestanding

TABLE I. Doping levels E_D, naphthalene desorption peak maximum $T_{\max}$, and binding energies E_b of naphthalene on graphene from experiment and theory in dependence of the intercalant. E_b^{exp} is given assuming $\nu = 5 \times 10^{16}$ Hz (without error, as it acts equally on all values).

	Experiment			Theory			
	E_D^{exp} (eV)	$T_{\max}$ (K)	E_b^{exp} (eV)	E_b^{tot} (eV)	E_b^{DFT} (eV)	E_b^{NL} (eV)	E_D^{theor} (eV)
Oxygen	+0.68[a]	233	−0.808	−0.806	0.366	−1.172	+0.88
Pristine	+0.10[b]	236	−0.819	−0.852	0.556	−1.408	+0.15
Europium	−1.36[c]	244	−0.848	−0.865	0.736	−1.601	−1.21

[a]Reference [36] (also Refs. [7] and [37]).
[b]Reference [38].
[c]Reference [8].

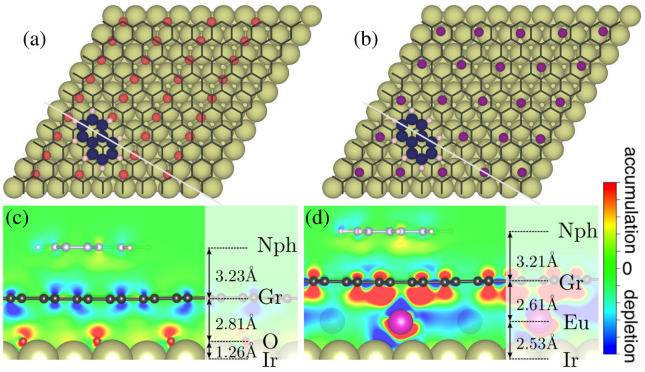

FIG. 3 (color online). Top view of relaxed adsorption geometries of naphthalene (Nph) on (a) O-intercalated and (b) Eu-intercalated graphene (Gr) on Ir(111). In (c) and (d), the corresponding plots of the charge density difference for each system are also presented. Color scale range is $\pm 5 \times 10^{-4} e/a_0^3$, with a_0 the Bohr radius.

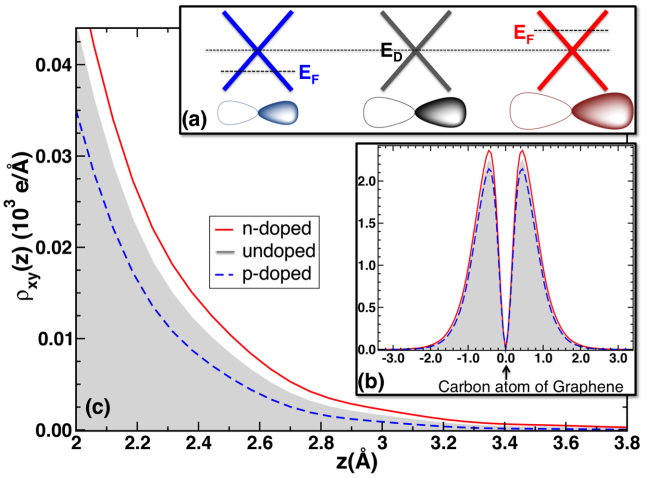

FIG. 4 (color online). (a) Schematic band structure near the Dirac point and representation of the π-orbital extension for p-doped, undoped, and n-doped graphene. (b) In-plane xy-integrated π-state charge density for (10×10) unit cells of freestanding graphene as a function of the z direction. (c) Zoom into the low-density tail of (b).

when intercalated with O or Eu [7,8], graphene on bare Ir(111) is slightly hybridized with its substrate in specific areas of its moiré [40]. This induces a certain modulation of E_b and, thus, renders the nonintercalated case less reliable. Second, the excellent match of the absolute values (within < 25 meV) of the binding energies must be considered fortuitous, as E_b extracted from thermal desorption data is expected to carry a larger systematic error. Unaffected by these two caveats, however, is the *difference* in E_b between the O- and Eu-intercalated cases, which, being ≈60 meV in the calculation and ≈40 meV in the experiment, matches reasonably well.

To gain an insight into the role of the vdW interactions in these systems, the total binding energy E_b^{tot} was decomposed into a DFT contribution E_b^{DFT} and a nonlocal one E_b^{NL} (for details, see Supplemental Material [30]), as seen in Table I. The data show that for all systems considered in our study, the DFT contribution E_b^{DFT} to E_b^{tot} is positive while the nonlocal one E_b^{NL} is negative; this indicates that the vdW interactions are indeed the driving force leading to a stable molecular adsorption. Furthermore, the magnitude of the attractive nonlocal contribution E_b^{NL} to the naphthalene binding significantly increases in the series from the O-intercalated (1.172 eV) via the pristine (1.408 eV) to the Eu-intercalated (1.601 eV) system.

To find out the reason for the modification of the vdW binding upon intercalation, we have conducted calculations on a freestanding graphene sheet of (10×10) unit cells. It was doped by directly adding or removing 0.05 electrons per C atom. To keep the calculated unit cell (on the whole) charge neutral, a balancing background charge had to be introduced. Figure 4(b) shows the resulting xy-integrated charge density for all π orbitals corresponding to the differently doped cases. As qualitatively illustrated in Fig. 4(c), the p or n doping of graphene results in a π charge density distribution that is less (p doped) or more (n doped) spatially extended as compared to that of the undoped graphene. A less (more) spatially extended π charge density corresponds to less (more) polarizable C atoms in the graphene layer and, therefore, will govern a weaker (stronger) vdW binding of the π adsorbates. This picture is derived from the behavior observed for the vdW bonded noble-gas dimers from He to Kr [41,42]. It is also backed up quantitatively by a recent analysis of Berland *et al.* [43], who found that, for benzene on graphene, most of the nonlocal energy in the vdW-DF arises from the extended regions of low charge density.

The increase in the nonlocal contribution with electron doping in Table I is mostly counteracted by the simultaneous increase in the repulsive DFT contribution, such that the total binding energy E_b^{tot} of the molecule to the surface is modified only slightly. Generally, in a pure vdW system, the attractive interaction forces have to be balanced by a counteracting Pauli repulsion force in any stable adsorption geometry. If one approximates the vdW contribution by the nonlocal correlation, one might tentatively attribute the increase in the repulsive DFT term to an additional Pauli repulsion as graphene's charge density becomes more extended due to n doping.

In view of the generality of the mechanism proposed above, we speculate that substitutional doping or tuning of the graphene Fermi level through a gate electrode will also affect the vdW contribution to the binding energy of adsorbates in a similar way. However, an effect of similar magnitude will likely require an electrolytic gate to obtain doping levels as large as those achieved by intercalation [44].

In conclusion, we find, with an excellent agreement of experiment and theory, an increase in the vdW binding energy of naphthalene to graphene, by about 5%, when

changing from p to n doping in the experimentally accessible range. Based on our DFT calculations, the graphene π orbitals become spatially more extended with n doping, making the space of low electron density between graphene and the molecule more polarizable, which in turn gives rise to a stronger vdW binding. The effect is robust with respect to changing either the intercalant or the molecule, and must, therefore, be assumed to provide a broadly applicable strategy to manipulate vdW binding in π-π systems.

The computations were performed under the auspices of the VSR at the computer JUROPA and the GCS at the high-performance computer JUQUEEN operated by the JSC at the Forschungszentrum Jülich. We gratefully acknowledge financial support from the Volkswagen-Stiftung through the "Optically Controlled Spin Logic" project (N. A. and V. C.), from the European Commission through a Marie Curie Fellowship (A. J. M.-G.), from the Institutional Strategy of the University of Cologne within the German Excellence Initiative (F. H.), from the Ministry of Education, Culture, Sports, Science and Technology of Japan (MEXT) through the "World Premier International Research Center Initiative" and the "Development of Environmental Technology using Nanotechnology" program (I. H.), and from the DFG Priority Program 1459 "Graphene" within Project No. MI581/20-1.

*huttmann@ph2.uni-koeln.de
†n.atodiresei@fz-juelich.de

[1] K. S. Novoselov, A. K. Geim, S. V. Morozov, D. Jiang, Y. Zhang, S. V. Dubonos, I. V. Grigorieva, and A. A. Firsov, Science **306**, 666 (2004).
[2] H. Wang, T. Maiyalagan, and X. Wang, ACS Catal. **2**, 781 (2012).
[3] A. Bostwick, F. Speck, T. Seyller, K. Horn, M. Polini, R. Asgari, A. H. MacDonald, and E. Rotenberg, Science **328**, 999 (2010).
[4] C. Coletti, C. Riedl, D. S. Lee, B. Krauss, L. Patthey, K. von Klitzing, J. H. Smet, and U. Starke, Phys. Rev. B **81**, 235401 (2010).
[5] C. Riedl, C. Coletti, T. Iwasaki, A. A. Zakharov, and U. Starke, Phys. Rev. Lett. **103**, 246804 (2009).
[6] M. Petrović, I. Šrut Rakić, S. Runte, C. Busse, J. T. Sadowski, P. Lazić, I. Pletikosić, Z.-H. Pan, M. Milun, P. Pervan, N. Atodiresei, R. Brako, D. Sokcević, T. Valla, T. Michely, and M. Kralj, Nat. Commun. **4**, 2772 (2013).
[7] R. Larciprete, S. Ulstrup, P. Lacovig, M. Dalmiglio, M. Bianchi, F. Mazzola, L. Hornekær, F. Orlando, A. Baraldi, P. Hofmann, and S. Lizzit, ACS Nano **6**, 9551 (2012).
[8] S. Schumacher, F. Huttmann, M. Petrović, C. Witt, D. F. Förster, C. Vo-Van, J. Coraux, A. J. Martínez-Galera, V. Sessi, I. Vergara, R. Rückamp, M. Grüninger, N. Schleheck, F. Meyer zu Heringdorf, P. Ohresser, M. Kralj, T. O. Wehling, and T. Michely, Phys. Rev. B **90**, 235437 (2014).
[9] V. W. Brar, R. Decker, H.-M. Solowan, Y. Wang, L. Maserati, K. T. Chan, H. Lee, Ç. O. Girit, A. Zettl, S. G. Louie, M. L. Cohen, and M. F. Crommie, Nat. Phys. **7**, 43 (2011).
[10] S. Schumacher, T. O. Wehling, P. Lazić, S. Runte, D. F. Förster, C. Busse, M. Petrović, M. Kralj, S. Blügel, N. Atodiresei, V. Caciuc, and T. Michely, Nano Lett. **13**, 5013 (2013).
[11] T. O. Wehling, B. Grundkötter-Stock, B. Aradi, T. Frauenheim, and T. Niehaus, Phys. Rev. B **90**, 085422 (2014).
[12] L. F. Huang, M. Y. Ni, G. R. Zhang, W. H. Zhou, Y. G. Li, X. H. Zheng, and Z. Zeng, J. Chem. Phys. **135**, 064705 (2011).
[13] S. D. Chakarova-Käck, E. Schröder, B. I. Lundqvist, and D. C. Langreth, Phys. Rev. Lett. **96**, 146107 (2006).
[14] R. Zacharia, H. Ulbricht, and T. Hertel, Phys. Rev. B **69**, 155406 (2004).
[15] E. Londero, E. K. Karlson, M. Landahl, D. Ostrovskii, J. D. Rydberg, and E. Schröder, J. Phys. Condens. Matter **24**, 424212 (2012).
[16] S. L. Tait, Z. Dohnálek, C. T. Campbell, and B. D. Kay, J. Chem. Phys. **125**, 234308 (2006).
[17] K. Berland, V. R. Cooper, K. Lee, E. Schröder, T. Thonhauser, P. Hyldgaard, and B. I. Lundqvist, Rep. Prog. Phys. **78**, 066501 (2015).
[18] R. van Gastel, A. T. N'Diaye, D. Wall, J. Coraux, C. Busse, N. M. Buckanie, F.-J. Meyer zu Heringdorf, M. Horn von Hoegen, T. Michely, and B. Poelsema, Appl. Phys. Lett. **95**, 121901 (2009).
[19] Provided by Ames Laboratory (Materials Preparation Center) of the US DOE, Iowa State University, Ames, Iowa 50011-3020, USA.
[20] Naphthalene "analytical standard" obtained from Sigma-Aldrich.
[21] I. Horcas, R. Fernández, J. M. Gómez-Rodríguez, J. Colchero, J. Gómez-Herrero, and A. M. Baro, Rev. Sci. Instrum. **78**, 013705 (2007).
[22] J. P. Perdew, K. Burke, and M. Ernzerhof, Phys. Rev. Lett. **77**, 3865 (1996).
[23] P. E. Blöchl, Phys. Rev. B **50**, 17953 (1994).
[24] G. Kresse and J. Hafner, Phys. Rev. B **47**, 558 (1993).
[25] G. Kresse and J. Furthmüller, Phys. Rev. B **54**, 11169 (1996).
[26] K. Lee, É. D. Murray, L. Kong, B. I. Lundqvist, and D. C. Langreth, Phys. Rev. B **82**, 081101 (2010).
[27] I. Hamada, Phys. Rev. B **89**, 121103 (2014).
[28] A. D. Becke, J. Chem. Phys. **85**, 7184 (1986).
[29] S. Schumacher, D. F. Förster, M. Rösner, T. O. Wehling, and T. Michely, Phys. Rev. Lett. **110**, 086111 (2013).
[30] See Supplemental Material at http://link.aps.org/supplemental/10.1103/PhysRevLett.115.236101, which includes Refs. [31–33], for the thermal desorption of naphthalene on additional intercalation systems, STM of benzene on intercalation-patterned graphene, and a description of the binding energy evaluation from DFT calculations.
[31] M. Petrović, Ph.D. thesis, University of Zagreb, 2014.
[32] P. Hohenberg and W. Kohn, Phys. Rev. **136**, B864 (1964).
[33] W. Kohn and L. J. Sham, Phys. Rev. **140**, A1133 (1965).
[34] A. J. Martínez-Galera, U. A. Schröder, F. Huttmann, W. Jolie, F. Craes, C. Busse, V. Caciuc, N. Atodiresei, S. Blügel, and T. Michely, Nanoscale, doi: 10.1039/C5NR04976H (2015).

[35] The 0.1-ML holes in graphene that are needed to intercalate O do not affect the obtained $T_{max} = 233$ K, since naphthalene desorbs at significantly higher temperatures from the hole area, i.e., from O-covered Ir(111).
[36] W. Jolie, F. Craes, M. Petrović, N. Atodiresei, V. Caciuc, S. Blügel, M. Kralj, T. Michely, and C. Busse, Phys. Rev. B **89**, 155435 (2014).
[37] S. Ulstrup, M. Andersen, M. Bianchi, L. Barreto, B. Hammer, L. Hornekær, and P. Hofmann, 2D Mater. **1**, 025002 (2014).
[38] I. Pletikosić, M. Kralj, P. Pervan, R. Brako, J. Coraux, A. T. N'Diaye, C. Busse, and T. Michely, Phys. Rev. Lett. **102**, 056808 (2009).
[39] R. F. W. Bader, *Atoms in Molecules–A Quantum Theory* (Oxford University Press, New York, 1990).
[40] C. Busse, P. Lazić, R. Djemour, J. Coraux, T. Gerber, N. Atodiresei, V. Caciuc, R. Brako, A. T. N'Diaye, S. Blügel, J. Zegenhagen, and T. Michely, Phys. Rev. Lett. **107**, 036101 (2011).
[41] M. Dion, H. Rydberg, E. Schröder, D. C. Langreth, and B. I. Lundqvist, Phys. Rev. Lett. **92**, 246401 (2004).
[42] D. Roy, M. Marianski, N. T. Maitra, and J. J. Dannenberg, J. Chem. Phys. **137**, 134109 (2012).
[43] K. Berland and P. Hyldgaard, Phys. Rev. B **87**, 205421 (2013).
[44] D. K. Efetov and P. Kim, Phys. Rev. Lett. **105**, 256805 (2010).